applied optics

Beam drift error and control technology for scanning beam interference lithography

Wei Wang,[1,2] Ying Song,[1] Shan Jiang,[1] Mingzhong Pan,[1] and Bayanheshig[1,*]

[1]National Engineering Research Centre for Diffraction Gratings Manufacturing and Application, Changchun Institute of Optics, Fine Mechanics and Physics, Chinese Academy of Sciences, Changchun Jilin 130033, China
[2]University of Chinese Academy of Sciences, Beijing 100049, China
*Corresponding author: bayin888@sina.com

Received 26 January 2017; revised 2 April 2017; accepted 12 April 2017; posted 13 April 2017 (Doc. ID 285587); published 8 May 2017

To improve the quality of grating masks made by scanning beam interference lithography, this article established a mathematical model of step-scanning exposure and analyzed the effects of the beam drift error on the interference image. Beam angle drift can be decomposed into the drift error δ_x in the exposure plane (XOZ plane) and the drift error δ_y perpendicular to the plane. Analysis shows that the δ_x has a major impact on the interference fringes during exposure, which may affect the precision of phase lock. δ_y leads to the appearance of deflected interference strips and affects the exposure dose. When a low-frequency drift error appears in the light path, the exposure contrast on the photoresist will decrease with the exposure process, which makes the fabrication of large-size diffraction gratings difficult. Furthermore, taking advantage of the characteristics of a scanning beam interference lithography system, an exposed beam stable system was designed that can effectively suppress the low-frequency drift of the beam. The total beam angle control accuracy is better than the 2.7 μrad, and position control accuracy is better than 3.9 μm (both for 1σ), which achieves the expected goal of the design.

OCIS codes: (050.2770) Gratings; (220.3740) Lithography; (220.4830) Systems design.

https://doi.org/10.1364/AO.56.004138

1. INTRODUCTION

Large-area holographic gratings are widely used in inertial confinement fusion laser driver systems. In the 1990s, to avoid static interference exposure in the production of large-area holographic gratings on lens materials and lens processing difficulties, researchers at the Massachusetts Institute of Technology (MIT) proposed a new method of making holographic gratings: scanning beam interference lithography (SBIL) [1–4]. Its principle is to make two Gaussian laser beams pass through the waist of a small-diameter optical system interference and by precise two-dimensional platform stepping-and-scanning, record the interference fringes in a substrate coated with a photoresist, thus fabricating a large-area grating mask. The SBIL technology is a blend of the characteristics of holographic gratings [5–7] and ruled gratings [8–10], and it can expose multiple fringes at the same time, although the interference images need to be precisely spliced. Because of the small-sized exposure, the SBIL technology has the advantages of high wavefront quality and uniformity of interference fringes. But the scanning beam interference lithography system is very complex, and the time large-grating production takes is long; it requires extreme precision conditions and control levels. Therefore, analyzing and controlling errors in the SBIL system is significant to the successful fabrication of large size gratings.

The SBIL technology is affected by the quality of the grating mask. An ideal grating mask should be prepared with a specific ratio and groove depth, and the bottom of the tank should be clean without residue on the sidewall of the rectangular groove. To date, there has been much fruitful work [11–14] on the relationship between the fabrication parameters of holographic grating masks and photoresist etching. Based on the development model of two-value photoresist [15], Montoya [1,16] at MIT has analyzed the influence of fringe period errors on the exposure contrast and discussed the relationship among contrast, exposure, and groove depth, given the tolerance of fringe period errors. However, there is little analysis of the effects of other errors on exposure in the SBIL system.

Because the SBIL technology adopts the stepping-and-scanning exposure mode, and the exposure time is longer, the laser beam will drift with time. There are three main factors that cause drift error: 1. the output beam of the laser has its own drift; 2. the laser and the optical system are on different foundations, so the difference in their vibrations leads to beam drift; and 3. the exposure light path is long, and many optical elements are arranged in the system, so the beam is prone to be

disturbed in the transmission process. The existence of beam drift error will lead to changes in the exposure parameters during the exposure process, resulting in a decrease in the uniformity of the mask and poor quality. Therefore, it is necessary to analyze the influence of the beam drift error in the stepping-and-scanning exposure process for the SBIL system.

This paper proposes a mathematical model for the effect of beam drift error on stepping-and-scanning exposure in the SBIL system and analyzes the influence of different drift errors on the system. It can provide theoretical guidance for the design of exposure systems and improve the quality of grating masks. At the same time, owing to the characteristics of the SBIL system, a beam stabilization system is designed that can suppress the beam drift error and meet the requirements of the exposure system.

2. SBIL SYSTEM EXPOSURE MODEL

The scanning beam interference lithography system creates an interference pattern using two collimated Gaussian beams at the waist; then, the precision platform drives the two-dimensional motion of the grating substrate and the interference fringes are exposed on the grating substrate coated with photoresist, as shown in Fig. 1(a). The direction of movement along the interference fringe is defined as the scanning direction (OY axis); the direction perpendicular to the interference fringe is defined as the step direction (OX axis). Because the energy distribution of the beam is a Gaussian distribution, to ensure the uniformity of exposure on the substrate during the exposure process, the energy needs to be partially overlapped in the two scanning directions. If the interference image waist radius on the substrate is ω, the step interval is usually $S = 0.8\omega$. The normalized exposure to overlap exposure is shown in Fig. 1(b); at this point, the uniformity of the exposure of the middle part is higher than 99.9%, which meets the demand for exposure uniformity.

A Gaussian beam is a plane in the beam waist position, and according to the Gaussian beam propagation formula, the complex amplitude distribution of the beam on the substrate can be

$$E_L = A \exp\left(-\frac{x^2+y^2}{\omega^2}\right) \exp\left(i2\pi \frac{\sin\theta}{\lambda} x\right), \quad (1)$$

$$E_R = A \exp\left(-\frac{x^2+y^2}{\omega^2}\right) \exp\left(i2\pi \frac{\sin\theta}{\lambda} x\right). \quad (2)$$

The intensity distribution of the interference field is formed after two-beam coherent superposition:

$$I(x,y) = I_L(x,y) + I_R(x,y) + 2\sqrt{I_L(x,y) I_R(x,y)} \cos\left(\frac{2\pi}{p} x + \varphi_0\right), \quad (3)$$

where A is a constant, ω is the waist radius, $I_L = |E_L|2$, $IL = |E_R|2$, and φ_0 is the initial phase. $p = \lambda/2 \sin\theta$ denotes the beam interference fringe period, where θ is half of the two-beam angle. The subscripts R and L in the formula represent the right and left laser beams, and this convention is also used below.

3. BEAM DRIFT ERROR ANALYSIS

A. Analysis of Beam Angle Drift Error

In the SBIL system, the Gaussian beam is emitted from the laser to the optical platform. To eliminate the influence of the laser's vibration on the exposure, the laser and the optical platform are usually removed, meaning there are some differences between the laser and optical platform, which will inevitably lead to the introduction of some drift to the laser beam.

A schematic diagram of SBIL is shown in Fig. 2. The exposure beam transmission plane is the XOZ plane. The interference fringe direction is perpendicular to the beam plane, which is the OY direction, and the interference pattern plane is the XOY plane. During the exposure process, one side of the exposure beam relative to the initial exposure beam has a certain angle drift φ, as shown in the dotted line in the figure.

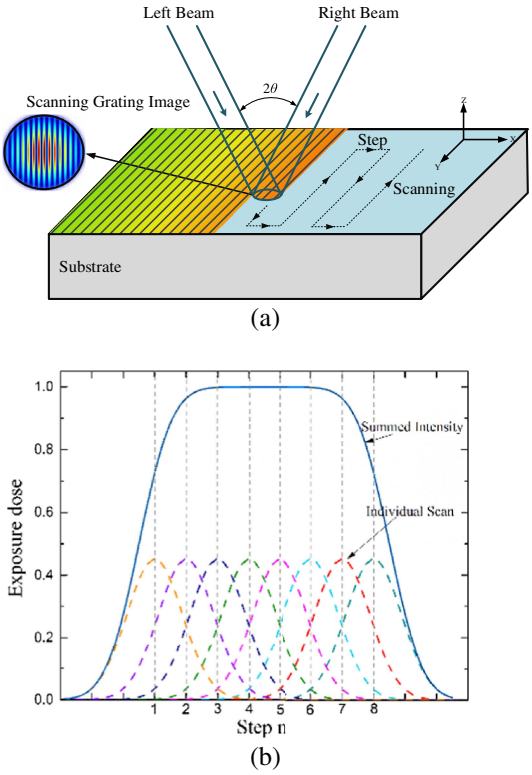

Fig. 1. Schematic diagram of the step-and-scanning exposure in SBIL.

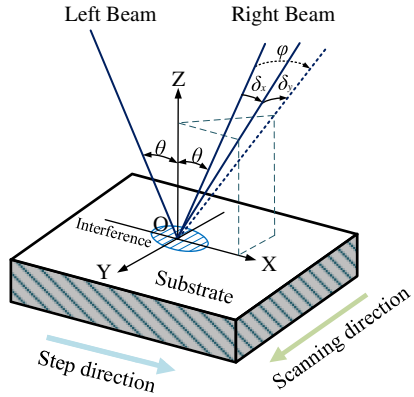

Fig. 2. Schematic diagram of the beam angle drift.

The influence of the angular drift in different directions on the system parameters is different, and system requirements for different parameters are not the same. For this reason, the angle drift is divided into the drift δ_x in the XOZ plane and the drift δ_y perpendicular to the XOZ plan. According to the spatial geometry: $\cos\varphi = \cos\delta_x \cos\delta_y$.

The variation of the beam angle δ_x in the XOZ plane has an influence on the period of the interference in the exposure process, which affects the precision of the fringe stitching. The drift δ_y, which is perpendicular to the XOZ plane, will lead to a certain deflection of the fringe direction, reduce exposure contrast during scanning, and broaden the line. Next, the effects of these two kinds of drift on the SBIL system will be analyzed in detail.

1. Influence of Angular δ_x on the Fringe Period

The SBIL system precision-stitches the fringes using phase-locking technology, which compensates for the phase change caused by substrate displacement using an acoustic optical modulator (AOM). The interference fringe period is the key parameter for the conversion between the substrate displacement and the grating phase in the phase-locking system. The period of interference fringe has shifted during the exposure, which means the benchmark of phase locking has changed; this would affect the grating mask groove. In this section, the influence of beam angle drift on the interference fringe period will be analyzed.

The two laser beams are incident on the grating substrate with wavelength λ, so the fringe period p can be obtained as follows:

$$p = \frac{\lambda}{2\sin\theta}. \tag{4}$$

The θ in the formula denotes the angle between the exposure beam and the grating substrate normal. In the process of making holographic gratings, the interference period can be adjusted by changing the angle between the two beams to achieve the purpose of making different line density gratings.

In the actual exposure system, because of the impact of the external environment, the exposure beam in the XOZ plane has an angle drift δ_x, as shown in Fig. 3, which represents the differential between the two ends of the formula (4):

$$\frac{dp}{p} = \frac{\lambda\cos\theta}{2p\sin^2\theta}d\theta. \tag{5}$$

According to the above analysis, the effects of beam angle drift δ_x on grating period were simulated, as shown in Fig. 4, in which the incident wavelength λ was 413.1 nm and values of

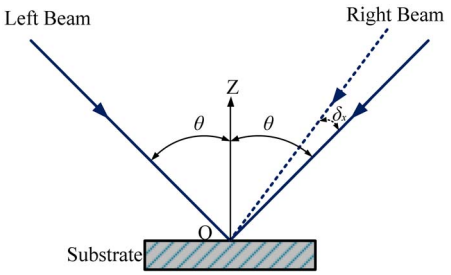

Fig. 3. Schematic diagram of the beam angle drift δ_x.

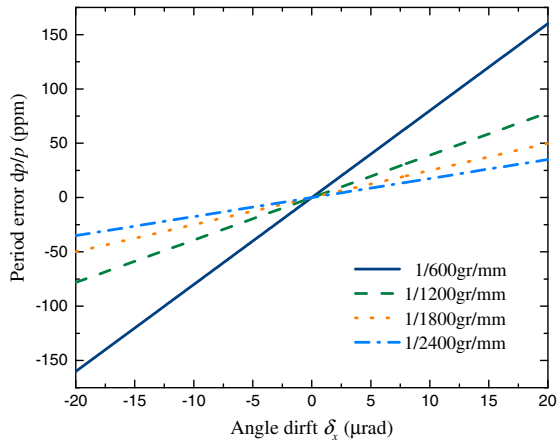

Fig. 4. Influence of beam angle drift on the fringe period.

the grating line density p were 1/600 gr/mm, 1/1200 gr/mm, 1/1800 gr/mm, and 1/2400 gr/mm.

The abscissa in the figure shows the variation of the beam angle δ_x in the XOZ plane. The ordinate represents the relative change in the interference period, with units of ppm. The following conclusions can be drawn from the figure:

(1) The period of the interference varies linearly with the beam angle drift; as the beam angle drift increases, the fringe period changes more sharply;

(2) Under different grating periods, the influence of beam angle drift on the fringe period is not the same; when the grating line density is small, the effect of beam angle drift on the fringe period is more obvious. This result means that larger grating periods require more stringent requirements for beam angle drift.

Specifically, with an exposure wavelength λ of 413.1 nm and a grating period p of 555.6 nm (1/1800 gr/mm), the precision of the grating period needed to keep within 10 ppm in the exposure process leads to a beam angle drift value of $\delta_x = \pm 4.005 \times 10^{-6}$ rad, which means that the beam angle drift should be controlled within ± 4 μrad.

2. Influence of Angle Drift δ_y on the Interference Direction and the Contrast

In the SBIL system, it is expected that the direction of interference fringes is strictly parallel to the scanning direction, to ensure the continuity of the latent image grating in the process of scanning. In fact, there is a certain angle between the interference fringe and the scanning direction; there is also a drift in the beam angle, leading to a change in the direction of the fringes. In this section, we will analyze the influence of the drift δ_y, which is perpendicular to the XOZ plane, on the direction of interference fringes and the exposure contrast.

For the laser beam in the transmission plane (XOZ plane), the direction vector of the left beam is $\boldsymbol{I_L}(0, \sin\theta, -\cos\theta)$, the direction vector of the right beam is $\boldsymbol{I_R}(0, -\sin\theta, -\cos\theta)$, and the direction vector of the interference fringes is $\boldsymbol{R}(1, 0, 0)$, as shown in Fig. 5. It is assumed that there is a drift δ_y perpendicular to the XOZ plane in the right side of the exposure beam, so the direction vector of the right beam is changed

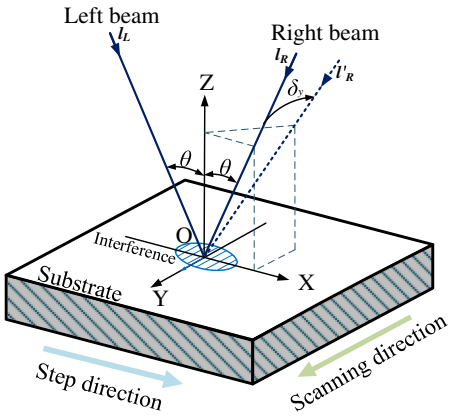

Fig. 5. Effect of angle drift δ_y on direction of interference fringes.

to $\boldsymbol{I'_R}(\sin\delta_y, -\cos\delta_y \sin\theta, -\cos\delta_y \cos\theta)$. At this time, the direction vector of the interference fringes is $\boldsymbol{R'}(\sin 2\theta \cos\delta_y, \cos\theta \sin\delta_y, \sin\theta \sin\delta_y)$, and it can be calculated that the direction change δ_i of the interference fringes in the XOY plane caused by the angular drift is

$$\tan\delta_i = \frac{\tan\delta_y}{2\sin\theta}. \tag{6}$$

Because of the existence of the beam angular drift δ_y, the direction of the interference fringe is deflected on the exposure plane. For example, when the exposure wavelength λ is 413.1 nm, the grating period p is 555.6 nm, and the exposure beam has a drift δ_y of 10 μrad; the direction of the interference fringes δ_i is 13 μrad.

The SBIL system uses the scanning exposure mode, limited to the precision of the guide rail and the adjustment precision of the fringe direction, so there exists an inherent declination δ_s between the interference fringe direction and the scanning direction. Therefore, the angle between the interference fringe direction and scanning direction is $\delta_\theta = \delta_s + \delta_i$ in the exposure process, as shown in Fig. 6.

Because there is an angle δ_θ between the fringe direction and the scanning direction, Eq. (3) becomes

$$I(x,y) = I_L(x,y) + I_R(x,y) + 2\sqrt{I_L(x,y)I_R(x,y)}\cos\left[\frac{2\pi}{p}(x+\delta_\theta y)+\varphi_0\right]. \tag{7}$$

During each scanning process, the substrate moves along the OY direction with a movement speed of v, so the amount of exposure on the substrate can be written as an integral of the interference fringe intensity:

$$D(x,y) = \int I(x,y,t)\mathrm{d}t. \tag{8}$$

Substituting Eq. (7) into the Eq. (8), we can obtain the expression for the exposure:

$$D(x,y) = \frac{\omega}{v}\sqrt{\frac{\pi}{2}}\exp\left(-2\frac{x^2}{\omega^2}\right)\left\{A_L^2 + A_R^2 + 2A_LA_R\exp\left[-\frac{1}{2}\left(\frac{\pi\omega\delta_\theta}{p}\right)\right]\cos\left(\frac{2\pi}{p}x\right)\right\}. \tag{9}$$

From the above equation, we can see that the exposure contrast after a single scanning exposure is

$$\gamma_0 = 2\frac{A_LA_R}{A_L^2+A_R^2}\exp\left[-\frac{1}{2}\left(\frac{\pi\omega\delta_\theta}{p}\right)\right]. \tag{10}$$

From Eq. (10), during the exposure process, because of the angle δ_θ between the interference fringe direction and the scanning direction, the exposure contrast decreases. Based on this analysis, we simulated the relationship between exposure contrast γ_0 and angular drift δ_y, as shown in Fig. 7. The fringe period p was 555.56 nm (1/1800 gr/mm), the inherent declination existing in the system was 20 μrad, and the beam waist radii were 1 mm, 1.5 mm, 2 mm, 2.5 mm, and 3 mm.

In the figure, the horizontal coordinate represents the angle δ_y, which is perpendicular to the XOZ plane, and the ordinate represents the exposure contrast γ_0 during a scanning exposure. The following conclusions can be drawn from the figure:

(1) The exposure contrast decreases with the beam angle drift δ_y; as the beam angle drift increases, the exposure contrast more sharply decreases;

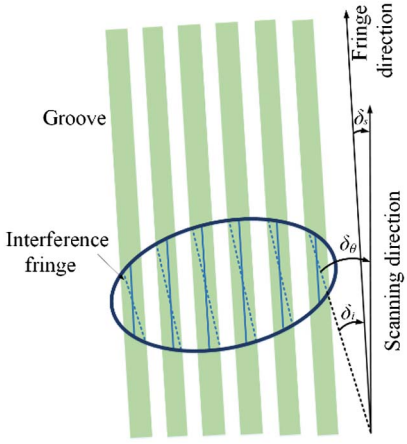

Fig. 6. Schematic diagram of the influence of the angle δ_θ between the fringe direction and the scanning direction on the scanning exposure.

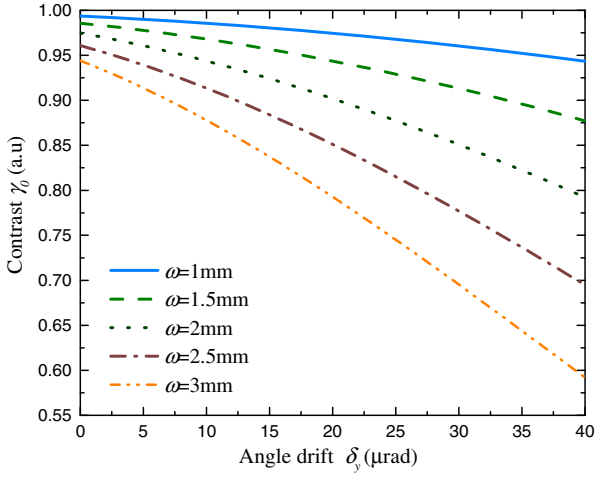

Fig. 7. Effect of angle drift δ_y on exposure contrast γ_0.

(2) Under different exposure spot sizes, the influence of beam drift on the exposure contrast is not the same. The larger the beam size is, the more obvious the effect of beam angle drift on the exposure contrast is; this is one of the advantages of a small-sized beam in the SBIL.

Specifically, for a period p of the grating of 555.6 nm (1/1800 gr/mm) and a beam waist radii ω of 1 mm, it is expected that exposure contrast fluctuations within 3% during the process will meet the requirements for etching with the grating mask. Based on the above analysis, it can be concluded that the angle drift δ_y perpendicular to the XOZ plane should be less than 15 μrad. If the size of the beam waist radii is 2 mm, the angular drift should be within 1.7 μrad.

B. Effect of Low-Frequency Linear Drift on the Exposure Contrast

The SBIL system uses a stepping-and-scanning exposure mode, so it requires a longer exposure time than static holographic exposure. To ensure the quality of the grating, the exposure status of the photoresist at different spatial positions needs to be consistent. In this section, we will analyze the effect of the low-frequency drift of the beam position on the exposure contrast during the whole exposure process.

It is assumed that there is a slow linear drift δ_p in the left side beam during the exposure process, and the drift rate is ζ, which means that the drift of the beam at exposure time t is $\delta_p = \zeta t$. Then, Eq. (3) is changed to

$$I(x,y,t) = I_{L\delta}(x,y) + I_R(x,y) + 2\sqrt{I_{L\delta}(x,y)I_R(x,y)}\cos\left(\frac{2\pi}{p}x + \varphi_1\right). \quad (11)$$

In this equation, $I_{L\delta} = \exp\{-2[(x+\varsigma t)^2 + y^2]/\omega\}$, where φ_1 represents the phase change caused by the beam drift. In the SBIL technique, the phase of the interference can be precisely controlled by phase locking, so the phase change of the interference introduced by the beam drift is not considered in this paper.

The stepping-and-scanning exposure mode is shown in Fig. 8. Assuming that each scan time is T, the scanning speed is v, and the step time is P; when scanning is to step n, the start time for the scan is $t_{n\_start} = (n-1)T + (n-1)P$ and the end time is $t_{n\_end} = nT + (n-1)P$.

Based on the above assumptions, the exposure of the nth step can be obtained:

$$D_n(x) = D_{Dn}(x) + D_{An}(x)\cos\left(\frac{2\pi}{p}x + \varphi_n\right). \quad (12)$$

D_{Dn} and D_{An} are

$$D_{Dn}(x) = \int_{t_{n\_start}}^{t_{n\_end}} [I_{L\delta}(x) + I_R(x)]vt\mathrm{d}t,$$

$$D_{An}(x) = \int_{t_{n\_start}}^{t_{n\_end}} [I_{L\delta}(x) + I_R(x)]vt\mathrm{d}t.$$

After the nth scanning step, the total exposure on the grating substrate is the sum of the n scanning exposures:

$$D(x) = \sum_{n=1}^{N} D_n(x) = \sum_{n=1}^{N} D_{Dn} + \sum_{n=1}^{N} D_{An}\cos\left(\frac{2\pi}{p}x + \varphi_n\right). \quad (13)$$

The first term in the equation indicates the average exposure of the photoresist, and the D_{An} frequency is much smaller than the interference fringe frequency, so the contrast of the total exposure on the photoresist can be expressed as

$$\gamma_N(x) = \sum_{n=1}^{N} D_{An} / \sum_{n=1}^{N} D_{Dn}. \quad (14)$$

Based on the above model, we simulated and discuss the exposure of photoresist under various conditions. The following parameters were used: grating size of 200 mm × 200 mm, scanning speed v of 10 mm/s, step interval S of 0.8 mm, step time P of 5 s, and number of steps n of 250 steps. The drift rates ζ were set to 0 μm/min, 1 μm/min, 3 μm/min, and 5 μm/min, respectively, and the contrast of the exposure on the whole photoresist was simulated as shown in Fig. 9.

The abscissa in Fig. 9 is the number of steps (the number of scans), and the ordinate is the total contrast of the substrate surface. The following conclusions can be drawn from the figure:

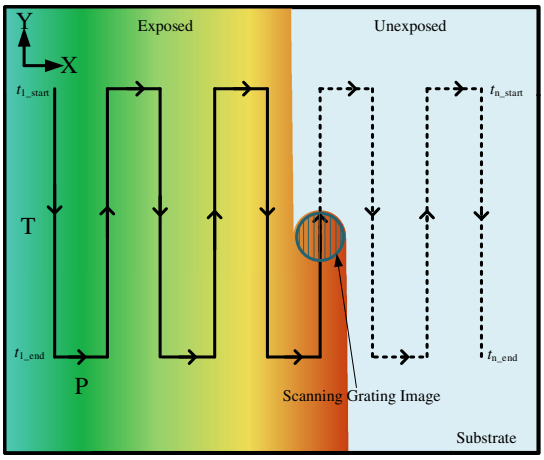

Fig. 8. Schematic diagram of stepping-and-scanning mode in the SBIL system.

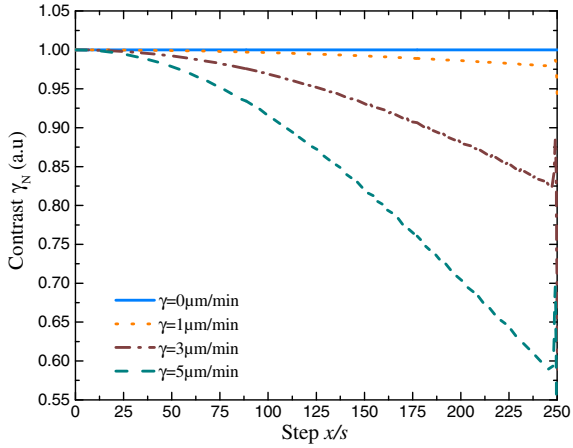

Fig. 9. Contrast on the photoresist under various drift rates.

(1) When the beam does not drift, the exposure contrast on the photoresist is an ideal exposure contrast of 1. At this time, the amount of bright stripes on the photoresist is sufficient, and the background light in the dark stripes is low. The removed photoresist is uniform with the retained photoresist, the depth of the grating mask groove is deep, and the side wall of the groove is steep. The quality of grating mask fabricated is the best.

(2) When low-frequency drift occurs in the optical path, the exposure contrast on the photoresist decreases with the exposure process. At the same number of steps, with increasing beam drift rate, there is a larger decrease in the exposure contrast on the photoresist. For example, when the drift rate is 3 μm/min, with approximately 96 steps, the exposure contrast decreased to below 0.97; with approximately 185 steps, the exposure contrast dropped below 0.9. When the exposure contrast decreases, the exposure of the bright stripes on the photoresist is not sufficient, and the photoresist removed on the grating substrate is not uniform. At this time, the grating mask groove is shallower and the non-uniformity of the grating surface is decreased. Therefore, the existence of low-frequency drift in the SBIL system is disadvantageous to the whole system performance. If the SBIL system is used to fabricate gratings with larger size, the time for grating fabrication will be further increased, and the harm caused by the low-frequency drift will continue to expand.

4. DESIGN AND EXPERIMENT OF BEAM STABILIZATION SYSTEM

A. Introduction to Beam Stabilization System

Based on the above simulation and analysis, combined with the characteristics of the SBIL optical path, a real-time beam stabilization system is designed, as shown in Fig. 10. The system consists of a laser light source, piezoelectric steering mirrors (FSM), reflectors, beam splitter (BS), polarizing beam splitter (PBS), decoupling lens, and two-dimensional position-sensitive detectors (PSD). When the beam is emitted by the laser, the angle and position of the beam can be adjusted by the two piezoelectric deflection mirrors. Then, the laser beam passes through the PBS and is divided into two beams. One beam is incident into the exposure light path, and the other beam enters the measurement apparatus of the beam stabilization system.

The angle and position of the beam are measured by a combination of the decoupling lens and the PSDs. One PSD is placed in the focal plane; the focal length of the lens is f_1, and the PSD measures the variation d_1, so the beam angle fluctuation can be obtained as $\alpha_1 = d_1/f$. Another PSD is placed in the l_2 position; the lens focal length is f_2, and when the change recorded by the PSD is d_2, the position of the light beam is $d_1 = d_2 f_2/(l_2 - f_2)$, which is the result of measurement of the beam position information.

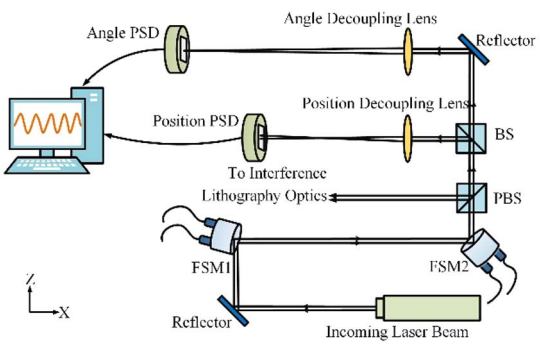

Fig. 10. Sketch of beam stabilization system for the SBIL.

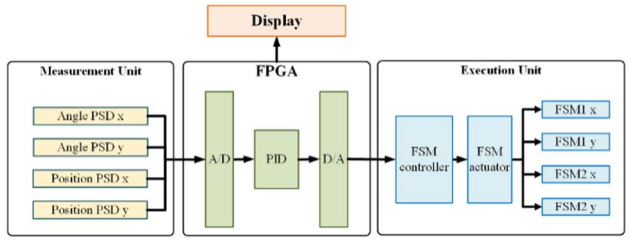

Fig. 11. Schematic diagram of the beam stabilizer controller.

The system has high real-time requirements for the control algorithm, so a field programmable gate array (FPGA) is selected to process the signal. The controller has 4 analog inputs, which acquire the angular and positional coordinates of the laser beam. There are 4 analog outputs of the controller, which control the 4 axes of the piezoelectric actuator, respectively. Figure 11 shows a schematic diagram of the beam stabilizer controller.

The PSD selected is a Newport OBP-U-9L. The focal length of the angle decoupling lens is 1000 mm, and the angle PSD is located on the focal plane. The position decoupling lens focal length is 100 mm, and the distance from the PSD to the lens is 150 mm. The A/D converter resolution is 16 bit and the input range is ±10 V, which means that the resolution is 0.305 mV. The PSD conversion relationship is 2.5 mV ⇒ 1 μm, that is, the PSD positional resolution is 0.122 μm. According to the principle of decoupling measurement, the resolution of the beam angle can be calculated as 0.122 μrad, and the resolution of the beam position is 0.244 μm. This design can clearly meet the measurement requirements for a beam stabilization system.

B. Experimental Results and Analysis

According to the above design, the beam stabilization system is set up in the SBIL system as shown in Fig. 12. The detector is

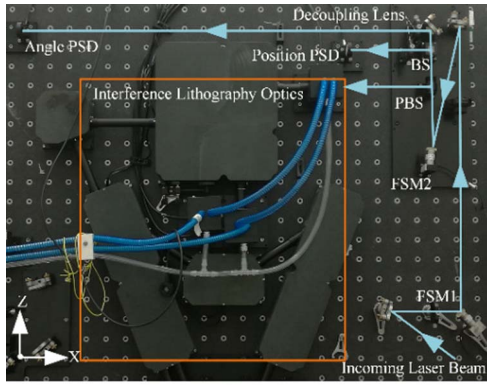

Fig. 12. Physical diagram of beam stabilization system.

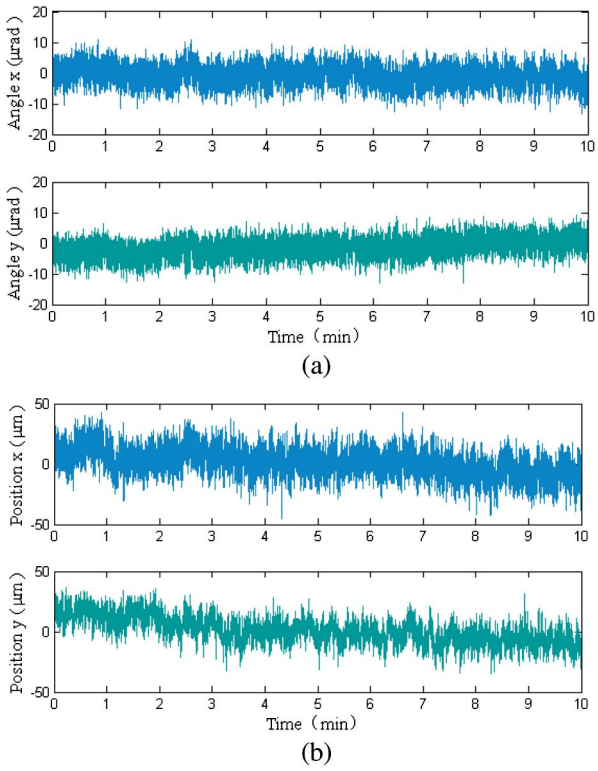

Fig. 13. Drift of an uncontrolled beam in the SBIL system.

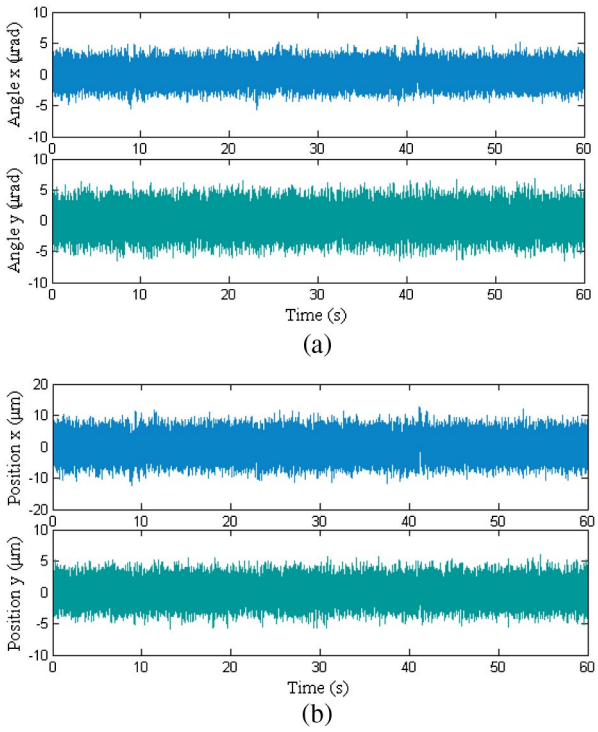

Fig. 14. Drift of a controlled beam in the SBIL system.

placed in the vertical optical path; the x direction of the detector is the OZ direction of the system, and the y direction of the detector is the OY direction.

Based on the design of the measurement system, we have tested the exposed beam uncontrolled; the measured frequency was 2 kHz, and the measurement time was 10 min (600 s), as shown in Fig. 13. Figure 13(a) represents the beam angle drift, and Fig. 13(b) indicates the beam position drift; the x direction corresponds to the blue curve in the figure, and the y direction corresponds to the green curve.

There is an obvious low-frequency drift phenomenon in the laser beam; in particular, the low-frequency drift of the beam position is obvious. The beam angle drift rate is approximately 0.3μrad/min, and the beam position drift rate is approximately 2.7 μm/min.

We have controlled the laser beam by the designed control system. Control results are shown in Fig. 14: (a) shows the beam angle stability results, and (b) shows the beam position stability results, where the x direction corresponds to the blue curve in the figure, and the y direction corresponds to the green curve.

The designed system can effectively suppress the low-frequency drift of the beam. The achieved beam angle stabilization accuracy is better than 1.4 μrad in the x direction and 2.3 μrad in the y direction, while the total angle control precision is better than 2.7 μrad. The beam position accuracy is better than 3.5 μm in the x direction, better than 1.6 μm in the y direction, and the total position control accuracy is better than 3.9 μm (both 1σ). Figure 15 shows the beam angle and position drift spectra; when the beam is uncontrolled, the low-frequency drift (less than 10 Hz) occupies a large proportion, and after the system is controlled, the low-frequency drift is well suppressed.

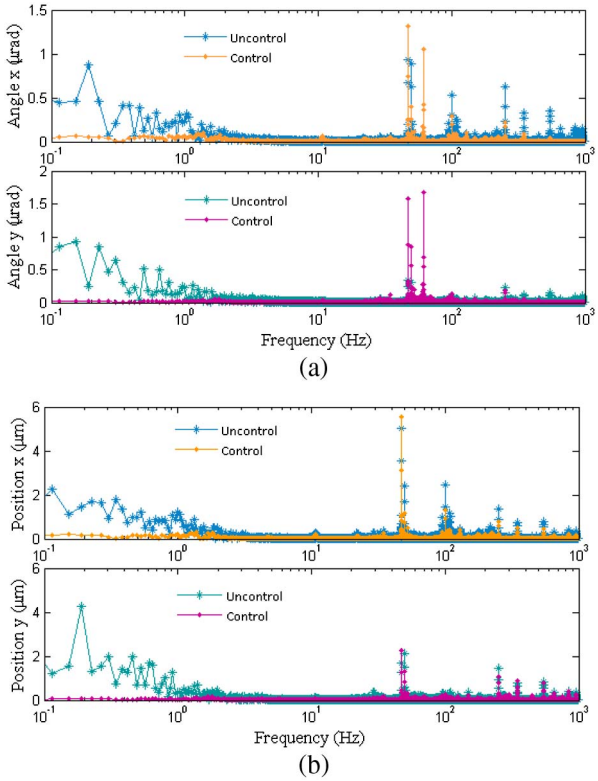

Fig. 15. Spectrum of beam drift.

5. CONCLUSIONS

In this paper, which studies the exposure beam of a SBIL system, a scanning exposure model with beam drift is established, and the influence of beam angle drift error and position drift error on the scanning exposure is analyzed. Then, based on the theoretical analysis, a beam stabilization system is designed. According to the simulation, analysis, and testing, the following conclusions can be drawn:

(1) The angle drift error can be decomposed into the drift δ_x in the XOZ plane and the drift δ_y perpendicular to the XOZ plane. The drift δ_x will have an impact on the fringe period and influence the fringe stitching accuracy. The drift δ_y will cause a deflection in interference fringe direction, reducing the exposure contrast in the scanning process. For a period p of 1/1800 gr/mm with a beam radius ω of 1 mm, to keep the grating measuring accuracy within 10 ppm, drift δ_x should be controlled within 4 μrad; to keep the exposure contrast fluctuations within 3%, the drift δ_y should be within 15 μrad.

(2) During the exposure process, the existence of low-frequency drift error leads to a decrease in the exposure contrast, an uneven exposure of the photoresist, and a decrease in the uniformity of the grating surface. If large gratings are fabricated, with the increased exposure time, the harm caused by low-frequency drift will continue to expand. Therefore, it is necessary to suppress the low-frequency drift error of the beam.

(3) An exposure beam stabilization system is designed for the SBIL that can effectively suppress the low-frequency drift of the beam. This system has achieved beam angle stabilization accuracy of better than 1.4 μrad in the x direction and 2.3 μrad in the y direction, with a total angle control precision of better than 2.7 μrad. The beam position accuracy is better than 3.5 μm in the x direction and better than 1.6 μm in the y direction, and the total position control accuracy is better than 3.9 μm (both 1σ). Therefore, the system has achieved the expected design objective.

Funding. National Key Scientific Instrument and Equipment Development Project of China (61227901).

REFERENCES

1. J. Montoya, *Toward Nano-Accuracy in Scanning Beam Interference Lithography* (Massachusetts Institute of Technology, 2006).
2. T. K. Paul, *Design and Analysis of a Scanning Beam Interference Lithography System for Patterning Gratings with Nanometer-Level Distortions* (Massachusetts Institute of Technology, 2005).
3. G. C. Chen, *Beam Alignment and Image Metrology for Scanning Beam Interference Lithography: Fabricating Gratings with Nanometer Phase Accuracy* (Massachusetts Institute of Technology, 2003).
4. Y. Bin, J. Wei, Z. Changhe, C. Hongsun, and S. Wenting, "Grating imaging scanning lithography," Chin. Opt. Lett. **11**, 080501 (2013).
5. A. Labeyrie and J. Flamand, "Spectrographic performance of holographically made diffraction gratings," Opt. Commun. **1**, 5–8 (1969).
6. M. Breidne, S. Johansson, L. E. Nilsson, and H. Ahlen, "Blazed holographic gratings," Opt. Acta **26**, 1427–1441 (1979).
7. H. Lin and L. F. Li, "Fabrication of extreme-ultraviolet blazed gratings by use of direct argon-oxygen ion-beam etching through a rectangular photoresist mask," Appl. Opt. **47**, 6212–6218 (2008).
8. X. T. Li, H. L. Yu, X. D. Qi, S. F. Feng, J. C. Chui, S. W. Zhang, Jirigalantu, and Y. G. Tang, "300 mm ruling engine producing gratings and echelles under interferometric control in China," Appl. Opt. **6054**, 1819–1826 (2015).
9. G. R. Harrison, S. W. Thompson, and H. Kazukonis, "750-mm ruling engine producing large gratings and echelles," J. Opt. Soc. Am. **62**, 751–756 (1972).
10. T. Kita and T. Harada, "Ruling engine using a piezoelectric device for large and high-groove density gratings," Appl. Opt. **31**, 1399–1406 (1992).
11. F. H. Dill, W. P. Hornberger, P. S. Hauge, and J. M. Shaw, "Characterization of positive photoresist," IEEE Trans. Electron Devices **22**, 445–452 (1975).
12. B. D. A. Mello, I. F. D. Costa, C. R. A. Lima, and L. Cescato, "Developed profile of holographically exposed photoresist gratings," Appl. Opt. **34**, 597–603 (1995).
13. C. Zanke, A. Gombert, and A. Erdmann, "Fine-tuned profile simulation of holographically exposed photoresist gratings," Opt. Commun. **154**, 109–118 (1998).
14. L. F. Li, *Application of Diffraction Theory to Analysis and Fabrication of Waveguide Gratings* (University of Arizona, 1988).
15. C. H. Chang, *Multilevel Interference Lithography–Fabricating Sub-Wavelength Periodic Nanostructures* (Massachusetts Institute of Technology, 2008).
16. J. C. Montoya, C. H. Chang, R. K. Heilmann, and M. L. Schattenburg, "Doppler writing and linewidth control for scanning beam interference lithography," J. Vac. Sci. Technol. B **23**, 2640–2645 (2005).